Microchemical Journal 195 (2023) 109481

Contents lists available at ScienceDirect

Microchemical Journal

journal homepage: www.elsevier.com/locate/microc

Low-cost colorimetric mercury sensor based on immobilisation of rhodamine B thiolactone in a sustainable agar-agar gel substrate

Klthom M. Nshnsh [a], Olga Cavoura [b], Christine M. Davidson [a,*], Lorraine T. Gibson [a]

[a] WestCHEM, Department of Pure and Applied Chemistry, University of Strathclyde, 295 Cathedral Street, Glasgow G1 1XL, UK
[b] Department of Public Health Policy, School of Public Health, University of West Attica, 196 Alexandras Avenue, Athens 11521, Greece

ARTICLE INFO

Keywords:
Rhodamine B thiolactone
Mercury
Water
Naked-eye colorimetric sensor
Sensor stability

ABSTRACT

The global impact of mercury (Hg) pollution requires the development of improved low-cost analytical sensors for Hg determination. Rhodamine B thiolactone (RBT) has been proposed as a colorimetric sensor for Hg^{2+} as it undergoes ring-opening in the presence of Hg to give a fast, reliable, and easily observed, colour change. In this study a naked-eye biopolymer-based sensor for Hg^{2+} detection was developed based on RBT-doped agar-agar membranes supported on filter papers. The chromogenic reagent was stable at −18 °C for over two years, whilst the RBT-doped sol–gel membranes prepared from 1% (*w/v*) agar colloid had a shelf-life of at least 12 weeks at room temperature when stored in the dark. The limit of detection (LOD) for naked-eye sensing was 0.4 μg L^{-1}. For Hg^{2+} quantification, images of the membranes were recorded using a flatbed scanner and analysed with public-domain ImageJ software. The linear range based on greyscale intensity in the green channel was 0.2–6.0 μg L^{-1} and the LOD was 0.2 μg L^{-1}. Precision was 10% (n = 3) and spike recoveries were in the range 97–103%. The sensors were regenerated using 10% *w/v* KI and successfully reused up to 4 times. Compared with other RBT-doped sol–gel sensors, the agar-agar membranes were simpler to prepare, more environmentally friendly, and gave a superior detection limit.

1. Introduction

Mercury is a pollutant of global concern [1,2]. It is emitted from various natural and anthropogenic sources, with small-scale gold mining and coal combustion being the largest anthropogenic contributors [3,4]. The toxic influence of Hg on human health is well documented [5,6]. The effects of Hg on human health depend on the level and duration of exposure, and the form of the element, since this influences the organ targeted. Symptoms of Hg toxicity include vomiting, severe abdominal pain, muscular weakness, headaches, mood swings, sleep disturbance, depression, and slowed nerve functions or memory loss. Permanent damage of the digestive system, kidneys and nervous system can results from chronic exposure [7].

The determination of Hg concentrations in environmental samples is necessary for contamination assessment and human health protection. However, particularly in resource-poor regions of the world (where the majority of activities such as small-scale gold mining take place) the use of classical methods of Hg detection is limited by high instrument costs and/or lack of instrument availability [8]. As a result, there has been considerable interest over the past decade in the development of Hg sensors. Ideally, such sensors would allow naked-eye identification in the field, without the need of additional reagents or equipment, at environmentally relevant guideline concentrations. In the case of drinking water, the World Health Organisation (WHO) guideline [9] for Hg is 6 μg L^{-1}, and the European Community (EC) maximum allowable concentration [10] is 1 μg L^{-1}. The United States Environmental Protection Agency has a limit [11] of 2 μg L^{-1} for drinking water, and has set freshwater and saltwater limits [12] at 1.4 μg L^{-1} and 1.8 μg L^{-1} respectively.

Small molecule sensors [13–22] have been used with some success for the detection of Hg in environmental samples. However, the majority of these sensors have not been adopted widely for reasons including lack of selectivity [23,24], poor aqueous solubility [25], or complicated synthetic routes [26,27]. Polymeric chemosensors can have several advantages over small molecules sensors including high thermal and mechanical stability, uniform polymeric pores, and easy diffusion of analyte ions [28]. However, additional steps and equipment are often necessary for application in the field [29–31]. Ready-to-use test strips or papers requiring no sample manipulation or additional equipment have also been proposed [32,33] although detection limits are poorer.

* Corresponding author.
E-mail address: c.m.davidson@strath.ac.uk (C.M. Davidson).

https://doi.org/10.1016/j.microc.2023.109481
Received 28 July 2023; Received in revised form 28 September 2023; Accepted 4 October 2023
Available online 9 October 2023

Rhodamines have been investigated as chemosensors for metal ions due to their high molar absorptivity, high fluorescence quantum yield and long wavelength absorption and emission [34]. Rhodamine B exhibits an equilibrium between two well-defined molecular forms; the lactone (L) and the zwitterion (Z) form (Fig. 1). Generally, the L form is colourless and has very weak absorption and emission bands, while the Z form is highly coloured [35,36].

Rhodamine B thiolactone (RBT) has been proposed as a simple and reliable chemosensor for naked-eye detection of trace Hg^{2+} in aqueous media. The sensing response is based on the ability of Hg^{2+} to induce ring-opening and trigger structural change from the colourless, non-fluorescent L form to the pink, fluorescent open Z form (Fig. 2) [37–39]. Naked-eye detection of Hg^{2+} at 2.0 μg L^{-1} has been achieved [40] using dispersive liquid–liquid microextraction to pre-concentrate Hg followed by reaction with RBT, and a more portable version of the same assay has been developed [39] that avoided the need to transport extractants to the field by using a RBT-doped sol–gel immobilised on a filter paper frit. In the sol–gel method the intensity of the colorimetric response is recorded using a flatbed scanner and Adobe Photoshop, achieving a detection limit of 0.24 μg L^{-1}. However, challenges were reported with stability of the sol–gel membranes, which developed a pink colour after exposure to air for 1 day. Although this could be mitigated by storing the membranes in 1.0 mM ascorbic acid or under nitrogen, slight colour change still occurred after 40 day. Further, the sol–gel preparation involves the use of harmful chemical substances such as tetraethyl orthosilicate, and hence is not in accordance with the principles of green analytical chemistry [41]. As a more environmentally friendly option, rhodamine functionalized cellulose was proposed as an Hg sensor [42]. While fluorometric response afforded an LOD of just under 0.2 mg L^{-1}, naked-eye detection was not possible below 1 mg L^{-1}.

Agar-agar is a natural, unbranched polysaccharide obtained from the cell wall of some species of red algae (*Rhodophyta*) that is made up of repeating units of D-galactose and 3,6-anhydro-L-galactopyranose. It is sustainable, biocompatible, non-toxic and relatively inexpensive. Its robust gelling ability and absence of interference with the reactivity of other bio-molecules have made agar-agar favourable for commercial applications in pharmaceutical, food and biotechnological industries [43–46]. Furthermore, the agar-agar colloid exhibits remarkable stability at temperatures up to 85 °C, even at concentrations as low as 0.1% [47].

This paper reports the successful development of a cheap, sustainable, robust Hg sensor based on RBT encapsulation within the polymeric network of agar-agar gel, and compares the performance of RBT-doped agar-agar with that of the established RBT-doped sol–gel for the colorimetric sensing of Hg^{2+} in water, using a flatbed scanner and ImageJ image processing software.

2. Experimental

2.1. Materials and methods

All regents were of analytical grade and used as received without further purification. Supplier information is as follows: Rhodamine B base - ACROS Organics, New Jersey, USA; sodium sulfide anhydrous (Na_2S) - Alfa Aesar, Lancashire, UK; tetraethyl orthosilicate (TEOS) - Sigma-Aldrich Company Ltd., Gillingham, UK; agar-agar, granular powder, - Fisher Scientific, Loughborough, UK; Whatman filter paper, (12.7 mm diameter, ashless, white ribbon) - GE Healthcare UK Ltd., Buckinghamshire, UK; acetonitrile (CH_3CN) - Sigma-Aldrich Company Ltd., Gillingham, UK; nitric acid (HNO_3) - Sigma-Aldrich Company Ltd., Gillingham, UK; and mercury (Hg^{2+}) 10,000 μg L^{-1} stock solution - QMX Laboratories Ltd, Essex, UK.

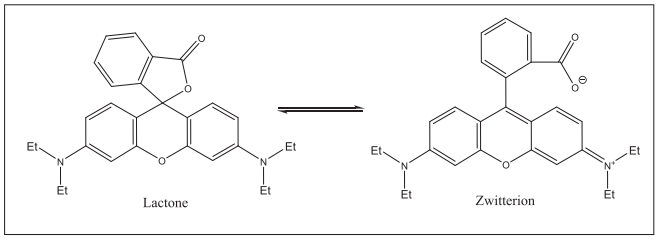

Fig. 1. Equilibria between lactone and zwitterion forms of rhodamine B.

Rhodamine B thiolactone was synthesised from rhodamine B base and Na_2S by a "one pot synthesis" route [37]. A stock solution of rhodamine B thiolactone (5 mM) was prepared in CH_3CN. Mercury stock solution was diluted in 2 % (*v/v*) HNO_3 as required.

2.2. Preparation of sensing gel membranes

The sol–gel membranes were prepared as described in Liu *et al.* [39]. The agar-agar colloid formulation was prepared by dissolving agar-agar powder in warm distilled water to give a concentration of 1% (*w/v*) agar. Once the resulting solution was a clear viscous liquid it was allowed to cool slightly before the addition of 5 mM RBT. The agar colloid and RBT solution were mixed in a 5:1 ratio for 2 min using a magnetic stirrer. Filter papers were dipped in the mixture, which was maintained at around 40 °C since the gel set if the temperature was allowed to fall below 25 °C, then withdrawn and dried in air for 30 min prior to use.

2.3. General procedure for colour development and data analysis

The Hg-sensing membranes were fixed in a 13 mm in-line polycarbonate filter holder and Hg standard solutions were pumped through the membranes at a flow rate of 17 mL min^{-1} using a multi-channel peristaltic pump (REGLO ICC, Cole-Parmer Ltd, UK). After colour development, the exposed sensors were removed from the holder and scanned immediately using a LiDE 220 flatbed scanner (Canon, UK). Chromogenic analysis was carried out based on the RGB colour model in greyscale mode using ImageJ software. ImageJ is a public-domain, Java-based, image processing programme developed at the United States National Institutes of Health, available to download at https://imagej.nih.gov/ij/.

3. Results and discussion

3.1. Stability of solid rhodamine B thiolactone

Rhodamine B thiolactone pale yellow crystals were synthesised with a 48% yield. A thiospirocyclic structure was confirmed by ^{1}H nmr and ^{13}C nmr spectroscopy, and by X-ray crystallography (see supplementary data). The solid was unstable under ambient conditions and began to change colour from yellow to pink within an hour of synthesis. This is consistent with the work of Liu *et al.* [39] who reported that oxidation of the RBT-based sol–gel membranes occurred rapidly in air. When observed under an optical microscope (Fig. 3) pink "branches" could clearly be seen developing around the edges of the pale yellow, needle-shaped RBT crystals, indicating that the transformation started from the outer layers, hence was induced by exposure to environmental factors.

To further investigate the stability of the synthesised chemosensor molecule, solid RBT was stored in sealed containers for up to two weeks in different environments: at ambient temperature in daylight; at ambient temperature in the dark; at −18 °C under white light; and at −18 °C in the dark. As shown in Fig. 4, the chemosensor changed colour under all conditions except when stored in the dark at −18 °C. This indicates that not only the presence of oxygen, but also the action of light and temperature, influence the equilibrium between the L and Z forms, and must be considered when assessing the suitability of RBT as a Hg^{2+} sensor under a range of conditions. No colour change from yellow to pink was observed at −18 °C in the dark even after storage for more

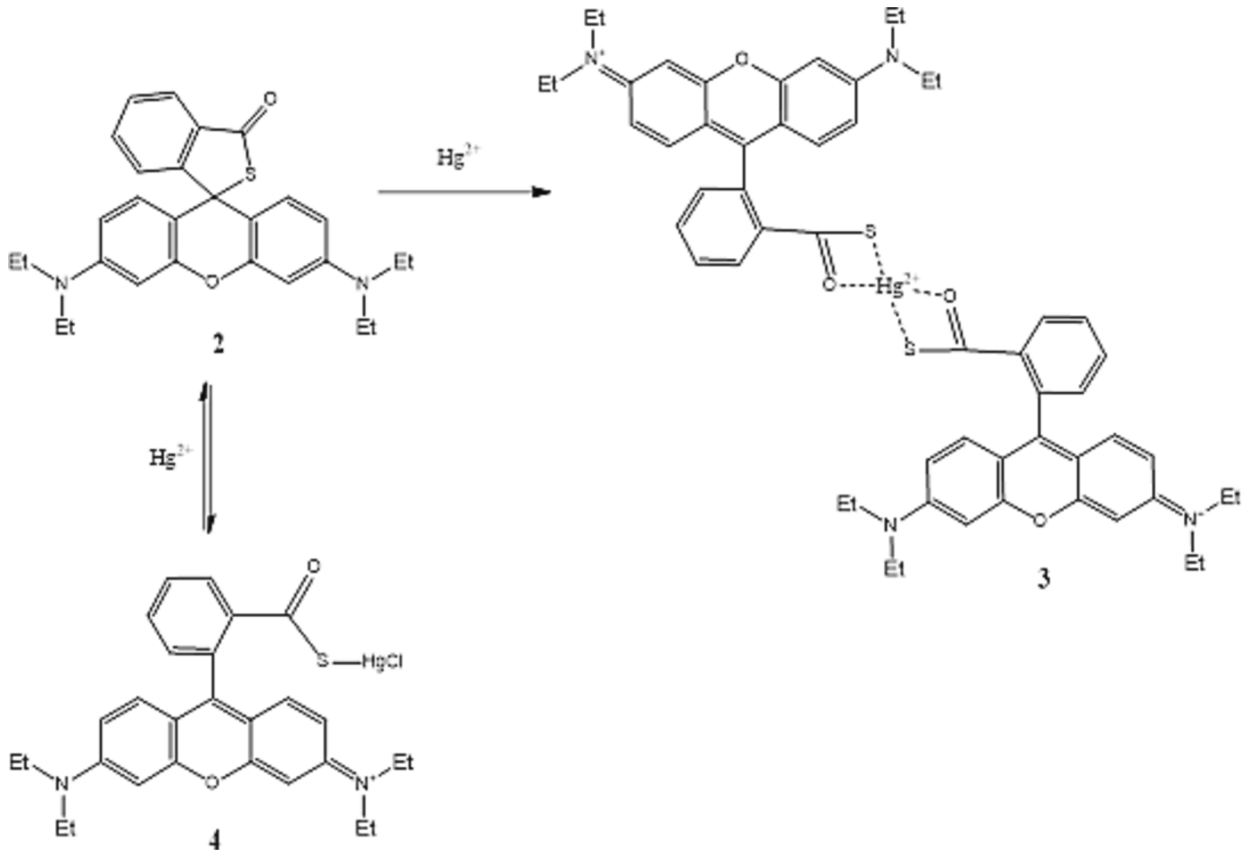

Fig. 2. The reaction between Hg^{2+} and rhodamine B thiolactone [37–39].

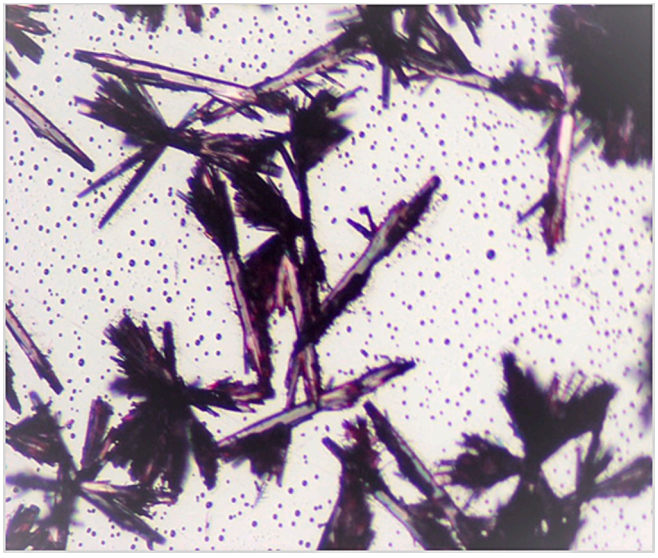

Fig. 3. Microscope photo of rhodamine B thiolactone crystals undergoing alteration.

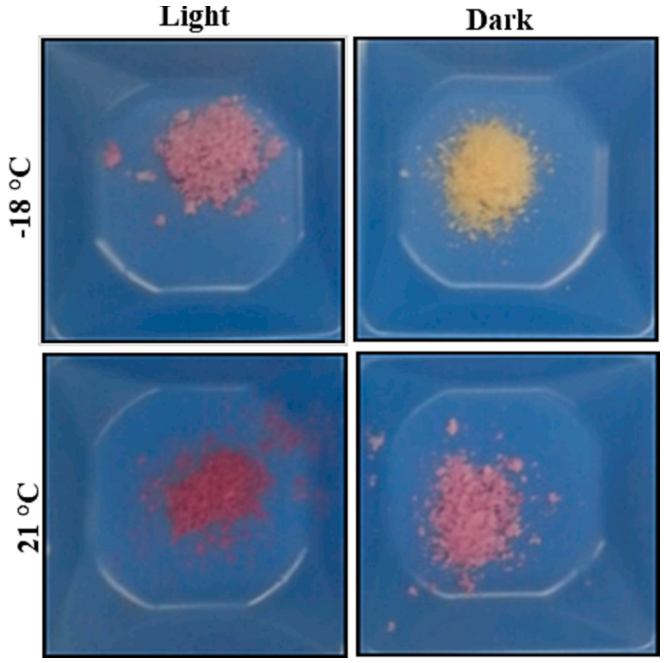

Fig. 4. Effect of storage conditions on the stability of solid rhodamine B thiolactone.

than 2 years. It was therefore concluded that solid RBT was stable when stored at low temperature and away from light. Bulk synthesis of an RBT solid is possible if the crystals produced are stored in the dark at −18 °C (i.e. in a freezer) before being used to prepare Hg^{2+} sensor membranes.

3.2. Interference study

Previous studies have demonstrated that RBT is relatively insensitive to non-analyte ions likely to be present in water samples. Zhan *et al.* [37] observed no colorimetric response in the presence of 5 μM of Ba^{2+}, Cd^{2+}, Co^{2+}, Cr^{3+}, Cu^{2+}, Fe^{3+}, Mn^{2+}, Ni^{2+}, Pb^{2+} or Zn^{2+} whilst Shi and Ma [38] reported no response when RBT was added to a mixed metal solution

containing 50 μM of Ca^{2+}, Cd^{2+}, Co^{2+}, Cu^{2+}, Fe^{3+}, K^{+}, Mg^{2+}, Mn^{2+}, Pb^{2+} and Zn^{2+}.

In the current study, no discernible colour change occurred in the presence of 5 mg L^{-1} of As^{3+}, Cd^{2+}, Co^{2+}, Cr^{3+}, Cu^{2+}, Fe^{3+}, Mg^{2+}, Mn^{2+}, Na^{+}, Ni^{2+}, Pb^{2+} and Zn^{2+}, but the RBT did give a weak response with Ag^{+} (Fig. 5a) as has been reported previously [38]. The colorimetric response for 1 mg L^{-1} Hg was similar in the presence, and in the absence, of the above mixture (Fig. 5b).

3.3. Chromogenic analysis of the colorimetric responses

When freshly prepared agar-agar membranes were exposed to standard solutions of Hg^{2+} the membrane changed colour from white to pink. Images of the sensors were recorded using a flatbed scanner and ImageJ software was used to decompose the image into red, green and blue components. To simplify data analysis and improve signal-to-noise ratio [48], the intensity in each channel was then converted to greyscale. As expected given the colour of the developed sensor ($\lambda_{MAX} = 559$ nm) the greyscale intensity in the green channel (G_G) gave the most distinct image (Fig. 6) and so was selected for further use. This is in agreement with previous work on sol–gel based RBT Hg^{2+} sensors that used a subtractive colorimetric detection approach [39].

3.4. Optimisation of sensing response on the agar-agar membrane

3.4.1. Selection of agar-agar gel colloid concentration

The mechanical properties of the RBT-doped agar-agar membranes could significantly affect their air and water permeability, hence their stability and suitability for use as Hg^{2+} sensors. To study these effects, agar colloids at concentrations of 1, 2, 3, 4 or 5% (*w/v*) were prepared and used to manufacture RBT-doped agar-agar membranes. A coating was successfully generated on the dipped filter paper in all cases. However, the membranes formed at higher colloid concentrations (4% or 5%) were hard and rigid after drying, while those formed from 1% and 2% colloid were soft and flexible. Slight rigidity was observed with the 3% colloid concentration. Further, the sensor papers prepared with higher concentrations of colloid began to curl as soon as the agar-agar dried, whilst those prepared with lower concentrations remained flat. The curvature of the sensor papers, which rendered them unsuitable for use, could be due to an increase in the intermolecular glycosidic bonds between the D- and L-galactose in the agar-agar matrix at higher concentration.

To investigate the air permeability of the agar-agar membranes and their protective ability to delay ring opening of immobilised RBT, membranes prepared with different concentrations of agar-agar colloid were exposed to ambient temperature and daylight. Sensor stability generally increased with increasing colloid concentration, presumably because the permeability of the gel decreased and so a longer time was required for penetration of air into the structure. Membranes prepared with 4% or 5% agar-agar began to show a pink tinge only after 3 w, those prepared with 2% or 3% agar-agar discoloured after 2 w, whilst those prepared with 1% agar-agar were stable for 1 w. Compared with the sol–gel membranes, which were stable for less than 1 day in contact with air [39], the agar-agar colloid protected the reagent from structural transformation well.

The mechanical flow characteristics of sensor membranes also influence their utility. A key requirement is to ensure high flow rates through the sensor in a reasonable timescale to ensure sufficient sensitivity. When water was pumped through the agar-agar membranes at a flow rate of 30 mL min^{-1} (as in Liu et al. [39]), it caused them to tear, regardless of the colloid concentration used in their preparation. When the flow rate was decreased to 17 mL min^{-1} no difficulty was experienced in passing water through the membranes prepared with 1, 2 or 3% agar-agar but those produced with 4% or 5% were virtually impermeable due to the development of high back pressures.

The membranes prepared with 1, 2 or 3% agar-agar colloid were further investigated in terms of the distribution of the coloured complex formed on exposure to Hg^{2+} solutions. Agar-agar membranes prepared with 1% colloid developed an even pink colour across the membrane, whereas 2 or 3% colloid membranes changed colour only at the edges of the membrane. Agar-agar membranes prepared with higher colloid concentrations also developed a slight 'dome-shape' as they rehydrated on contact with sample solution. When this occurred, the Hg^{2+} standard solution flowed preferentially through the thinner edges of the membrane impacting on the sensing platform. In contrast, membranes prepared with a 1% agar-agar colloid had a uniform thickness allowing water to easily permeate the entire surface area of the sensor, allowing for higher sensitivity of response due to a greater interaction of Hg^{2+} with immobilised RBT. Therefore a flow rate of 17 mL min^{-1} and sensor membrane prepared from 1% (*w/v*) agar-agar colloid were chosen for further study.

3.4.2. Assessment of water sample volume flowing through agar-agar membranes

The concentration of Hg^{2+} present will dictate the volume of water that needs to be passed through the agar-agar membranes, with lower

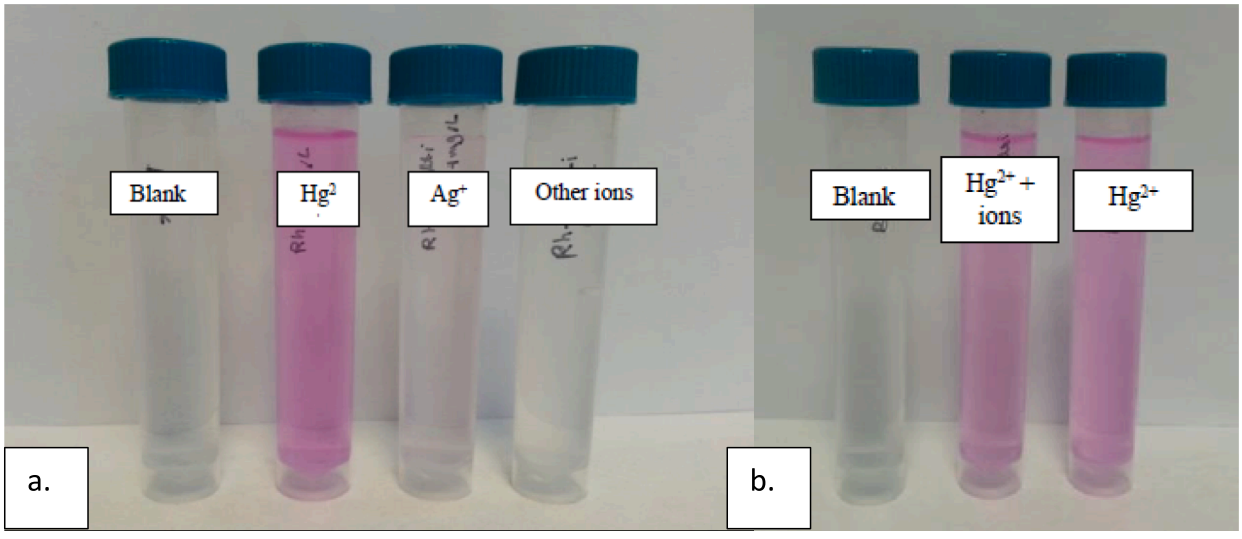

Fig. 5. Effect of potential interferents (a) colorimetric response for Hg^{2+}, Ag^{+} and a mixture containing 5 mg L^{-1} of As^{3+}, Cd^{2+}, Co^{2+}, Cr^{3+}, Cu^{2+}, Fe^{3+}, Mg^{2+}, Mn^{2+}, Na^{+}, Ni^{2+}, Pb^{2+} and Zn^{2+} (b) colorimetric response for Hg alone and in the presence of the mixture.

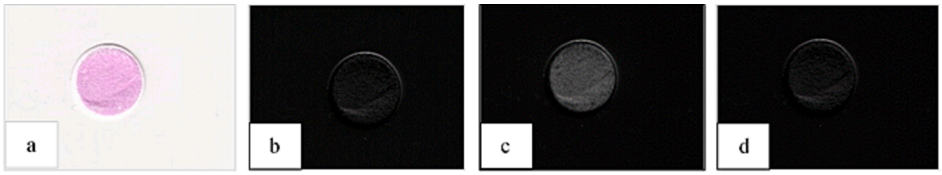

Fig. 6. Images of a filter paper coated with RBT-doped agar-agar colloid after exposure to Hg^{2+}. (a) the original image, (b) grey in red channel (G_R), (c) grey in green channel (G_G) and (d) grey in blue channel (G_B). (For interpretation of the references to colour in this figure legend, the reader is referred to the web version of this article.)

concentrations requiring higher volumes of water to be detected. To estimate the sample volume required to provide sensitive detection of Hg^{2+}, standard solutions containing 5 or 10 μg L^{-1} Hg^{2+} were studied. Different volumes of each solution – from 50 to 1000 mL – were passed through agar-agar membranes and the greyscale intensity in the green channel recorded. As shown in Fig. 7, and observed previously for sol–gel based membranes [39], the initial linear response in colour change quickly plateaued. The shape of the curve may indicate an initial rapid reaction of Hg^{2+} with the more accessible RBT molecules close to the exposed surface of the membrane followed by slower saturation of less accessible sites. The sample volume could be adjusted depending on the desired detection range of Hg^{2+}. However, considering the sensitivity and the appropriate linear range for Hg^{2+} at such low concentration, a sample volume of 300 mL was selected for further use.

3.4.3. Assessment of colorimetric reagent

To minimise sensor costs, the minimum amount of colorimetric reagent required to detect Hg^{2+} at typical environmental concentrations should be used. An experiment was conducted where different amounts of 5 mM RBT solution (0.5, 1.0, 1.5 or 2.0 mL, corresponding to 2.5×10^{-6}, 5.0×10^{-6}, 7.5×10^{-6} and 1.0×10^{-5} mole of RBT, respectively) were added to 5 mL of 1% (*w/v*) agar-agar colloid. The membranes were then exposed to 300 mL of either 5 or 10 μg L^{-1} Hg^{2+} solution (Fig. 8). Statistical analysis (ANOVA at 0.05 significance level) indicated that there was no significant difference in colour intensity between the sensors prepared with different amounts of RBT for the lower Hg^{2+} concentration, but there was significant difference at 10 μg L^{-1} Hg^{2+}. To identify which sensor(s) gave a different response, a series of t-tests at 0.05 significance level were carried out, which indicated that the result for the membrane prepared with 0.5 mL of RBT solution was dissimilar to the others. This may be because the amount of RBT available was insufficient to react with all of the Hg^{2+} present in the sample. A 300 mL aliquot of 10 μg L^{-1} Hg^{2+} solution contains 15 nmole of Hg. Given that between 60 and 80 sensor papers could be prepared from the 5.5 mL of doped colloid containing 2.5×10^{-6} mole of RBT, it can be estimated that around 37 nmole of the chromogenic reagent was likely to be present in each sensor. However, some of this may have been located within closed pores inaccessible to the Hg^{2+} solution. Since use of the minimum amount of reagent was desirable, it was decided to prepare sensors by adding 1 mL of RBT solution to 5 mL of colloid.

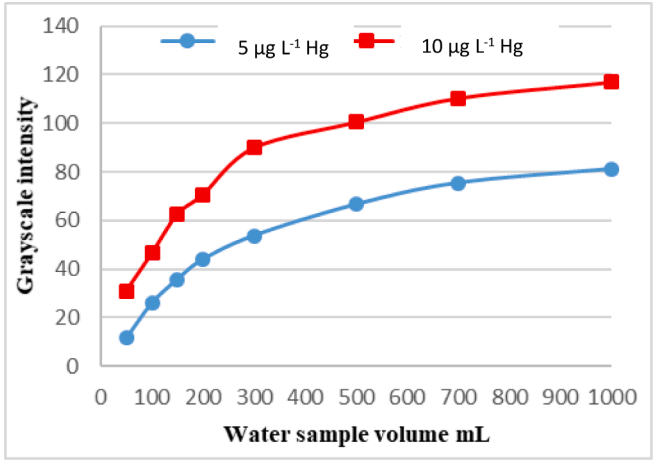

Fig. 7. Effect of sample volume on the colorimetric response in the G_G of the RBT-doped agar-agar sensor. The concentration of rhodamine B thiolactone in the agar membrane was 5.0×10^{-6} mol. Error bars represent one standard deviation (n = 3).

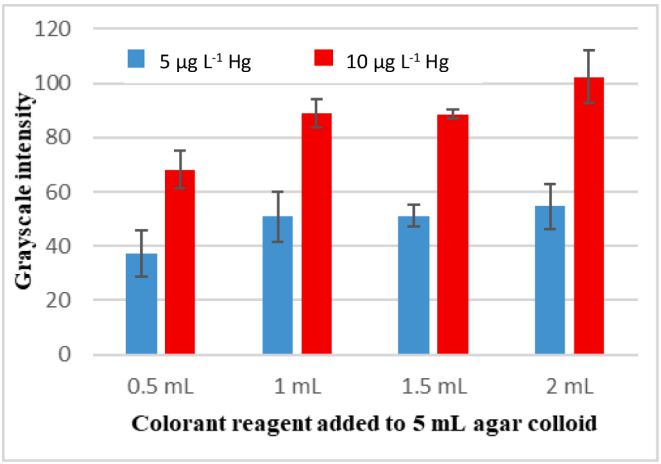

Fig. 8. Influence of colorant reagent volume on the colorimetric response in the G_G of the RBT-doped agar-agar sensor. The concentrations of rhodamine B thiolactone in the agar membranes were 2.5×10^{-6}, 5.0×10^{-6}, 7.5×10^{-6} and 1.0×10^{-5} mol. Error bars represent one standard deviation (n = 3).

3.5. Analytical performance

A fit-for-purpose Hg^{2+} sensor must be able to detect the analyte at environmentally-relevant concentrations. For the agar-agar membrane, the colour change (white to pink) could be discriminated clearly by the naked eye at 0.4 μg L^{-1} Hg^{2+}, below the water quality and drinking water guidelines (Fig. 9). Thus the sensor could for be used for both pollution monitoring and health protection without the need for additional sample preparation or instrumentation.

Mercury standard solutions with concentration from 0.2 to 20 μg L^{-1} were prepared and 300 mL aliquots analysed in triplicate to assess the linear range of the agar-agar membrane response. As expected, the G_G value increased with Hg^{2+} concentration (Fig. 10). A linear correlation ($r^2 = 0.990$) was found over the range 0.2–6 μg L^{-1}, which encompasses Hg concentrations likely to be present except in highly contaminated waters. The instrumental limit of detection was 0.2 μg L^{-1} at which concentration the precision (RSD) for analysis of three replicate agar-agar membranes was 11.5%.

The accuracy of the proposed agar-agar method was evaluated by spike recovery tests carried out at three concentration levels in triplicate. The initial Hg^{2+} concentration was 1 μg L^{-1} and the spiked concentrations were 1, 3 or 5 μg L^{-1}. The spiked sample solutions were pumped through the sensors, then the exposed membranes were

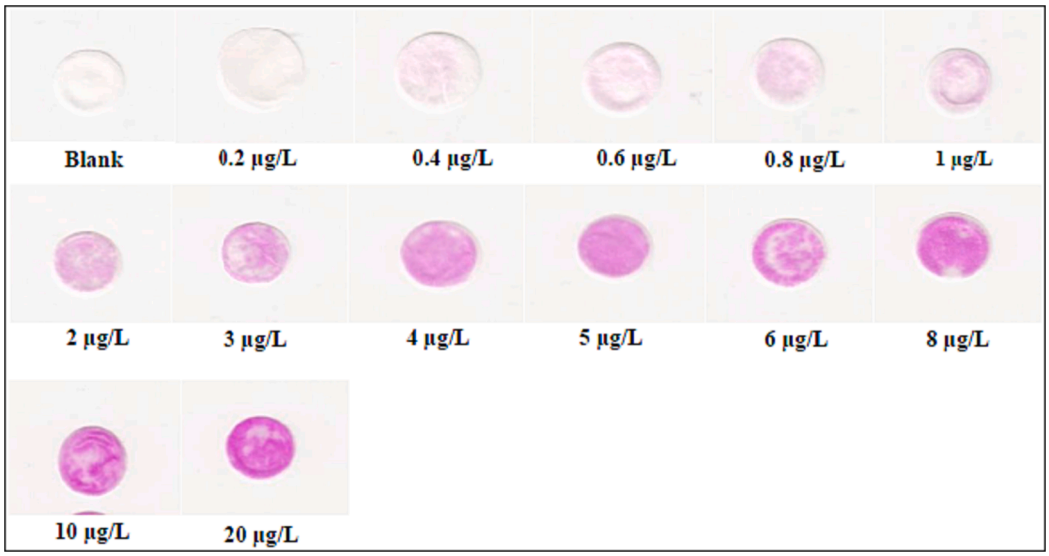

Fig. 9. Sequential increase in the colour intensity of the agar-agar membrane with increasing Hg^{2+} concentration.

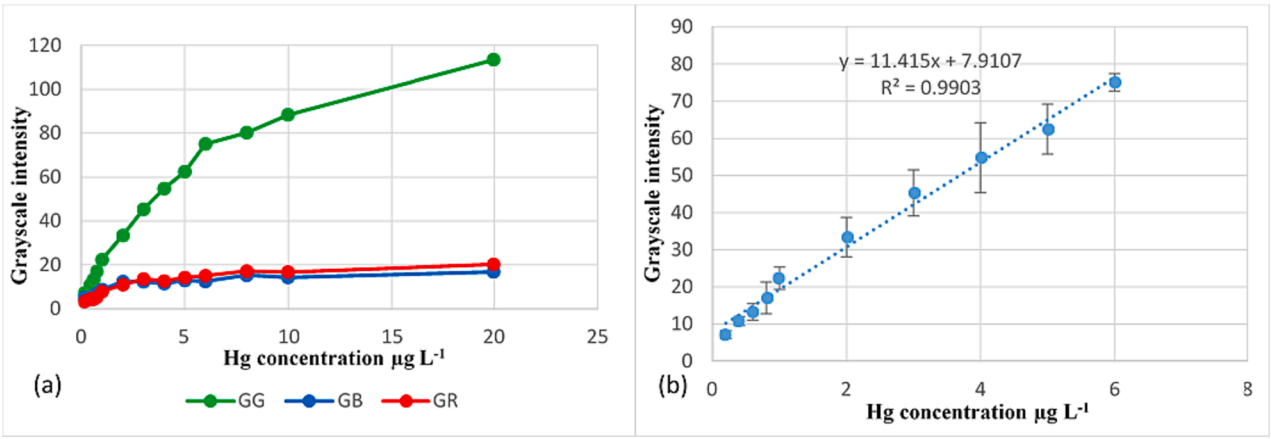

Fig. 10. The relationship between the colorimetric response in G_R, G_G and G_B and the concentration of Hg^{2+} on the exposed RBT-doped agar-agar gel membranes. (a) 0–20 µg L^{-1} Hg^{2+}, (b) linear correlation in the concentration range from 0.2 to 6 µg L^{-1}; Error bars represent one standard deviation (n = 3).

scanned for chromogenic analysis. After the intensities in G_G were measured, the Hg^{2+} concentrations were obtained from the corresponding regression equations and the initial concentration subtracted to obtain the spike recovery values in Table 1. Recoveries were 99.1%, 103% or 97.7% for the low, medium and high spike concentration levels, respectively. The RSD values were less than 10% in all cases.

3.6. Membrane stability and reactivity following storage

As discussed in Section 3.1, RBT is likely to undergo ring opening under ambient conditions, giving rise to a pink colour even in the absence of Hg^{2+}. Hence, the stability of the sensor membrane needs to be evaluated at ambient temperature, in the daylight, and in the dark. In addition, some of the agar-agar membranes were 'capped' with a protective layer of 5% (*w/v*) agar-agar – which had to be peeled off before the sensor was used – to investigate whether this would extend the shelf-life. The agar-agar membrane showed no colour change when kept in the dark for 12 weeks at room temperature, and was stable for up to 1 week in the daylight (Fig. 11). The addition of a 5% agar-agar film over the surface of the doped membrane did increase the length of time the agar-agar membrane could tolerate ambient conditions, but only for a period of up to 2 weeks after which time a pale pink colour developed.

Table 1
Spike recovery results for the agar-agar membranes based on the response in the G_G channel.

Initial Hg^{2+} µg L^{-1}	Hg^{2+}Added µg L^{-1}	Hg^{2+} Found µg L^{-1} n = 3	% Recovery ± % RSD n = 3
1	1	1.990 ± 0.089	99.1 ± 9.04
1	3	4.09 ± 0.144	103 ± 4.65
1	5	5.89 ± 0.438	97.7 ± 8.98

Results are mean ± SD; n = number of replicates.

For comparison, sol–gel membranes were prepared and stored under various conditions: at ambient temperature in the daylight and in the dark; at ~ 4 °C in a refrigerator; in 0.1 mM ascorbic acid solution (as recommended by Liu et al. [39] and in a tightly sealed bottle containing sachets of oxygen absorber (Oxygen Absorber Ageless®, Mitsubishi Gas Chemical Company, Inc.). As expected, the sol–gel membranes exposed to ambient conditions became pink after just 1 day (after 1 week in the dark or in ascorbic acid). Because the acid catalysed sol–gel membranes cured rapidly, they were prone to the formation of small cracks. This may have increased their air permeability. Sol-gel membranes were however stable for up to 12 week when stored at low temperature or kept free from oxygen.

The reactivity of both types of sensors was tested following storage

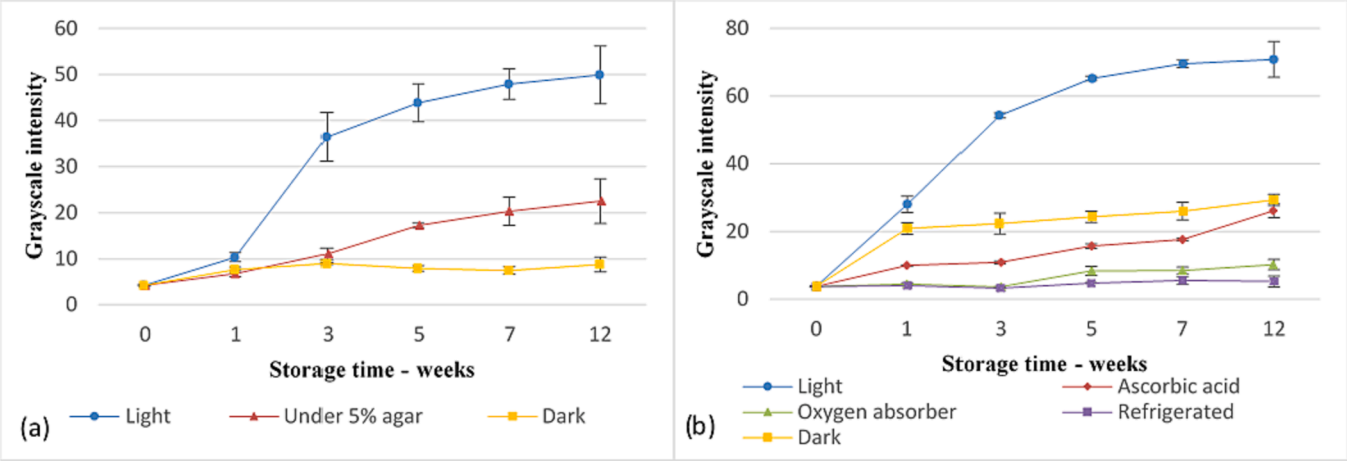

Fig. 11. Stability of RBT-doped (a) agar-agar and (b) sol–gel membranes stored under different condition. Error bars represent one standard deviation (n = 3).

for up to 12 weeks (Fig. 12). Only those sol–gel membranes stored away from oxygen or at low temperature gave similar colour intensity to freshly-prepared sensors. In contrast, it was only necessary to store agar-agar membranes away from light to maintain their performance. Simpler storage requirements are a clear advantage for a sensor intended for field use in resource-poor areas. Agar-agar membranes could, for example, simply be wrapped (or supplied pre-packaged) in foil for transport to the field, rather than requiring refrigeration or the addition of oxygen absorbers, as would be the case for sol–gel membranes.

3.7. *Recycling of agar-agar membrane with KI*

An investigation into the re-usability of the agar-agar membranes was conducted by exposure of the membrane to 10 μg L^{-1} Hg^{2+} (to generate an easily detectable pink colour) followed by dropwise addition of 10% *w*/v KI to the membrane surface, reversing the colour change. This could be repeated several times (Fig. 13) indicating the development of a reusable sensor membrane.

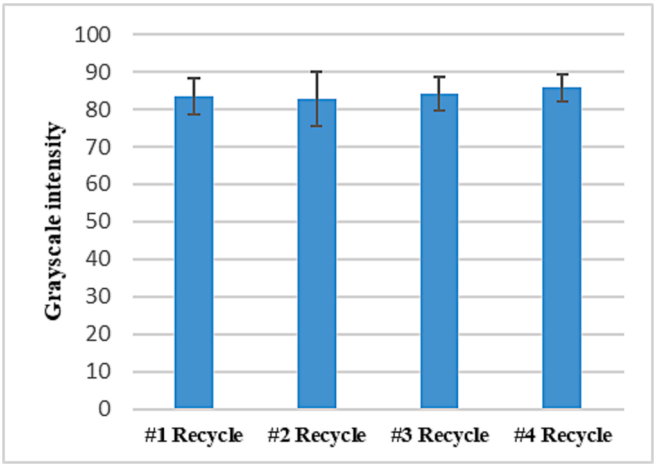

Fig. 13. Recycling of RBT-doped agar-agar membranes. In each cycle, the membranes were exposed to 10 μg L^{-1} Hg^{2+}, then treated with a solution of KI. Error bars represent one standard deviation (n = 3).

4. Conclusion

A naked eye membrane sensor for the detection of Hg^{2+} in water samples has successfully been developed based on RBT immobilised in agar-agar supported on filter paper. Quantitative determination of Hg^{2+} was achieved by chromogenic analysis using a flatbed scanner and public-domain software. The sensors could be stored for at least 12 weeks in the dark, and sensors were re-usable following regeneration with 10% *w*/v KI. Limits of detection were 0.4 μg L^{-1} (naked-eye) and 0.2 μg L^{-1} (digital image analysis) lower than current legislative thresholds for Hg^{2+} in drinking water. The linear range was 0.2–6.0 μg L^{-1} and spiked recovery values were 100 ± 3%. Compared with the previously reported RBT-doped sol–gel membrane sensors, the

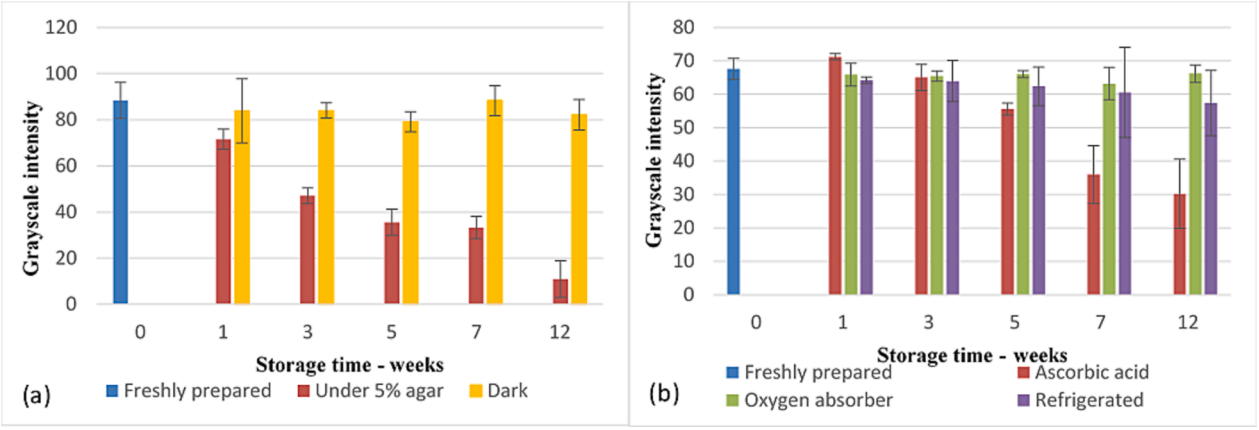

Fig. 12. Reactivity of RBT-doped (a) agar-agar and (b) sol–gel membranes after storage for up to 12 weeks. The membranes were exposed to 10 μg L^{-1} Hg^{2+} solution. Error bars represent one standard deviation (n = 3).

preparation of the proposed agar-agar membranes was simpler, used less harmful reagents, had lower limits of detection and a significantly longer shelf-life when stored in the dark. Further work to migrate the chromogenic detection to a mobile phone-based platform, adapting the method to field application, and application to real environmental samples, is required.

CRediT authorship contribution statement

Klthom M. Nshnsh: Conceptualization, Formal analysis, Funding acquisition, Investigation, Writing – original draft. **Olga Cavoura:** Writing – review & editing. **Christine M. Davidson:** Resources, Supervision, Writing – review & editing. **Lorraine T. Gibson:** Supervision, Writing – review & editing.

Declaration of Competing Interest

The authors declare that they have no known competing financial interests or personal relationships that could have appeared to influence the work reported in this paper.

Data availability

Data will be made available on request.

Acknowledgements

KMN acknowledges the financial support of the Libyan Ministry of Higher Education and Scientific Research. The authors wish to thank Dr Mark Spicer for assistance with synthesis of the RBT, and Dr Alan Kennedy/the UK National Crystallography Service for X-ray analysis. OC wishes to thank the University of West Attica, Greece, for approving the sabbatical leave that enabled collaboration in the study.

Appendix A. Supplementary data

Supplementary data to this article can be found online at https://doi.org/10.1016/j.microc.2023.109481.

References

‡ *Crystal data for rhodamine B thiolactone: the unit cell was found to match that in the literature.*

[1] F.M.M. Morel, A.M.L. Kraepiel, M. Amyot, The chemical cycle and bioaccumulation of mercury, Annu. Rev. Ecol. Syst. 29 (1) (1998) 543–566, https://doi.org/10.1146/annurev.ecolsys.29.1.543.
[2] R.P. Mason, A.L. Choi, W.F. Fitzgerald, C.R. Hammerschmidt, C.H. Lamborg, A. L. Soerensen, E.M. Sunderland, Mercury biogeochemical cycling in the ocean and policy implications, Environ. Res. 119 (2012) 101–117.
[3] UNEP. United Nations Environment Programme (2013). Global Mercury Assessment 2013: Sources, emissions, releases, and environmental transport. https://wedocs.unep.org/20.500.11822/7984. Published online 2013.
[4] U.N. Environment, Global Mercury Supply, Trade and Demand (2017). http://wedocs.unep.org/bitstream/handle/20.500.11822/21725/global_mercury.pdf?sequence=1&isAllowed=y.
[5] B. Fernandes Azevedo, L. Barros Furieri, F.M. Peçanha, G.A. Wiggers, P. Frizera Vassallo, M. Ronacher Simões, J. Fiorim, P. Rossi de Batista, M. Fioresi, L. Rossoni, I. Stefanon, M.J. Alonso, M. Salaices, D. Valentim Vassallo, Toxic effects of mercury on the cardiovascular and central nervous systems, J. Biomed. Biotechnol. 2012 (2012) 1–11.
[6] R.A. Bernhoft, Mercury toxicity and treatment: A review of the literature, J. Environ. Public Health 2012 (2012) 1–10, https://doi.org/10.1155/2012/460508.
[7] S. Bose-O'Reilly, K.M. McCarty, N. Steckling, B. Lettmeier, Mercury exposure and children's health, Curr. Probl. Pediatr. Adolesc. Health Care 40 (8) (2010) 186–215.
[8] WHO. Mercury and health. http://www.who.int/mediacentre/factsheets/fs361/en/. Published online 2017.
[9] WHO. *Guidelines for Drinking-Water Quality, 4th Edition.*; 2017.
[10] European Commission, COUNCIL DIRECTIVE 98/83/EC of 3 November 1998 on the quality of water intended for human consumption, Off. J. Eur. Commun. 41 (1998) 32–54.
[11] US EPA, National Primary Drinking Water Regulations, United States Environmental Protection Agency, Washington, DC, 2009.
[12] US EPA, National Recommended Water Quality Criteria - Aquatic Life Criteria Table, United States Environmental Protection Agency, Washington, DC, 2022.
[13] E.M. Nolan, S.J. Lippard, Tools and tactics for the optical detection of mercuric ion, Chem. Rev. 108 (9) (2008) 3443–3480, https://doi.org/10.1021/cr068000q.
[14] R.K. Mahajan, R. Kaur, V. Bhalla, M. Kumar, T. Hattori, S. Miyano, Mercury(II) sensors based on calix[4]arene derivatives as receptor molecules, Sensors Actuators, B Chem. 130 (1) (2008) 290–294, https://doi.org/10.1016/j.snb.2007.08.006.
[15] M.B. Gholivand, M. Mohammadi, M.K. Rofouei, Optical sensor based on 1,3-di(2-methoxyphenyl)triazene for monitoring trace amounts of mercury(II) in water samples, Mater. Sci. Eng. C 30 (6) (2010) 847–852, https://doi.org/10.1016/j.msec.2010.03.021.
[16] J. Liu, M. Yu, X.-C. Wang, Z. Zhang, A highly selective colorimetric sensor for Hg2 + based on nitrophenyl-aminothiourea, Spectrochim. Acta A Mol. Biomol. Spectrosc. 93 (2012) 245–249, https://doi.org/10.1016/j.saa.2012.03.021.
[17] A.R. Firooz, A.A. Ensafi, K. Karimi, R. Khalifeh, Specific sensing of mercury(II) ions by an optical sensor based on a recently synthesized ionophore, Sensors Actuators B Chem. 185 (2013) 84–90, https://doi.org/10.1016/j.snb.2013.04.108.
[18] K. Bera, A.K. Das, M. Nag, S. Basak, Development of a rhodamine–rhodanine-based fluorescent mercury sensor and its use to monitor real-time uptake and distribution of inorganic mercury in live zebrafish larvae, Anal. Chem. 86 (5) (2014) 2740–2746, https://doi.org/10.1021/ac404160v.
[19] D. Shi, F. Yan, M. Wang, Y.u. Zou, T. Zheng, X. Zhou, L.i. Chen, Rhodamine derivative functionalized chitosan as efficient sensor and adsorbent for mercury(II) detection and removal, Mater. Res. Bull. 70 (2015) 958–964.
[20] S.Y. Lee, J.J. Lee, K.H. Bok, J.A. Kim, Y.K. So, C. Kim, A colorimetric chemosensor for the sequential recognition of Mercury (II) and iodide in aqueous media, Inorg. Chem. Commun. 70 (2016) 147–152, https://doi.org/10.1016/j.inoche.2016.06.004.
[21] Q. Zhang, J. Zhang, H. Zuo, C. Wang, Y. Shen, A novel near-infrared chemosensor for mercury ion detection based on D-A structure of triphenylamine and benzothiadiazole, Tetrahedron 73 (19) (2017) 2824–2830, https://doi.org/10.1016/j.tet.2017.03.088.
[22] C.H. Jeon, C.S. Park, C.S. Lee, T.H. Ha, Simple immobilization of mercury ion chemosensors to solid substrate, J. Ind. Eng. Chem. 57 (2018) 370–376, https://doi.org/10.1016/j.jiec.2017.08.045.
[23] S.M. Park, M.H. Kim, J.-I. Choe, K.T. No, S.-K. Chang, Cyclams bearing diametrically disubstituted pyrenes as Cu^{2+} - and Hg^{2+} -selective fluoroionophores, J. Org. Chem. 72 (9) (2007) 3550–3553, https://doi.org/10.1021/jo062516s.
[24] K.P. Prathish, D. James, J. Jaisy, R.T. Prasada, Dual optoelectronic visual detection and quantification of spectroscopically silent heavy metal toxins: A multi-measurand sensing strategy based on Rhodamine 6G as chromo or fluoro ionophore, Anal. Chim. Acta 647 (1) (2009) 84–89, https://doi.org/10.1016/j.aca.2009.04.044.
[25] G. Zhang, D. Zhang, S. Yin, X. Yang, Z. Shuai, D. Zhu, 1,3-Dithiole-2-thione derivatives featuring an anthracene unit: New selective chemodosimeters for Hg(II) ion, Chem. Commun. 6 (16) (2005) 2161–2163, https://doi.org/10.1039/b417952h.
[26] E. Palomares, R. Vilar, J.R. Durrant, Heterogeneous colorimetric sensor for mercuric saltsElectronic supplementary information (ESI) available: Materials and methods. See http://www.rsc.org/suppdata/cc/b3/b314138a/, *Chem Commun*. (4) (2004) 362.
[27] S. Yoon, A.E. Albers, A.P. Wong, C.J. Chang, Screening mercury levels in fish with a selective fluorescent chemosensor, J. Am. Chem. Soc. 127 (46) (2005) 16030–16031, https://doi.org/10.1021/ja0557987.
[28] N. Choudhury, B. Saha, P. De, Recent progress in polymer-based optical chemosensors for Cu2+ and Hg2+ Ions: A comprehensive review, Eur. Polym. J. 2021 (145) (2020), 110233, https://doi.org/10.1016/j.eurpolymj.2020.110233.
[29] Y. Zhu, Y. Cai, Y. Zhu, L. Zheng, J. Ding, Y. Quan, L. Wang, B. Qi, Highly sensitive colorimetric sensor for Hg2+ detection based on cationic polymer/DNA interaction, Biosens. Bioelectron. 69 (2015) 174–178.
[30] T. Savran, S.N. Karuk Elmas, D. Aydin, S. Arslan, F.N. Arslan, I. Yilmaz, Design of multiple-target chemoprobe: "naked-eye" colorimetric recognition of Fe3+ and off–on fluorogenic detection for Hg2+ and its on-site applications, Res. Chem. Intermed. 48 (3) (2022) 1003–1023, https://doi.org/10.1007/s11164-021-04648-8.
[31] Y. Shan, W. Yao, Z. Liang, L. Zhu, S. Yang, Z. Ruan, Reaction-based AIEE-active conjugated polymer as fluorescent turn on probe for mercury ions with good sensing performance, Dye Pigment. 156 (February) (2018) 1–7, https://doi.org/10.1016/j.dyepig.2018.03.060.
[32] V. Sicilia, P. Borja, M. Baya, J.M. Casas, Selective turn-off phosphorescent and colorimetric detection of mercury(ii) in water by half-lantern platinum(ii) complexes, Dalt Trans. 44 (15) (2015) 6936–6943, https://doi.org/10.1039/c5dt00087d.
[33] N.A. Azmi, S.H. Ahmad, S.C. Low, Detection of mercury ions in water using a membrane-based colorimetric sensor, RSC Adv. 8 (1) (2018) 251–261, https://doi.org/10.1039/c7ra11450h.
[34] M. Beija, C.A.M. Afonso, J.M.G. Martinho, Synthesis and applications of Rhodamine derivatives as fluorescent probes, Chem. Soc. Rev. 38 (8) (2009) 2410, https://doi.org/10.1039/b901612k.

[35] A.A. El-Rayyes, A. Al-Betar, T. Htun, U.K.A. Klein, Fluorescence emission from rhodamine-B lactone adsorbed at solid catalysts, Chem. Phys. Lett. 414 (4–6) (2005) 287–291, https://doi.org/10.1016/j.cplett.2005.07.099.
[36] C.J. Stephenson, K.D. Shimizu, A fluorescent diastereoselective molecular sensor for 1,2-aminoalcohols based on the rhodamine B lactone–zwitterion equilibrium, Org. Biomol. Chem. 8 (5) (2010) 1027, https://doi.org/10.1039/b918823a.
[37] X.-Q. Zhan, Z.-H. Qian, H. Zheng, B.-Y. Su, Z. Lan, J.-G. Xu, Rhodamine thiospirolactone. Highly selective and sensitive reversible sensing of Hg(ii), Chem. Commun. 16 (2008) 1859, https://doi.org/10.1039/b719473k.
[38] W. Shi, H. Ma, Rhodamine B thiolactone: a simple chemosensor for Hg2+ in aqueous media, Chem. Commun. 16 (2008) 1856, https://doi.org/10.1039/b717718f.
[39] J. Liu, D. Wu, X. Yan, Y. Guan, Naked-eye sensor for rapid determination of mercury ion, Talanta 116 (2013) 563–568, https://doi.org/10.1016/j.talanta.2013.07.035.
[40] J. Liu, D. Wu, C. Duan, Y. Guan, Dispersive liquid–liquid microextraction of trace Hg2+ for visual and fluorescence test, Talanta 105 (2013) 87–92, https://doi.org/10.1016/j.talanta.2012.11.061.
[41] A. Gałuszka, Z. Migaszewski, J. Namieśnik, The 12 principles of green analytical chemistry and the SIGNIFICANCE mnemonic of green analytical practices, TrAC Trends Anal. Chem. 50 (2013) 78–84, https://doi.org/10.1016/j.trac.2013.04.010.
[42] N. Kolarova, P. Napiórkowski, Ecohydrology & Hydrobiology Trace elements in aquatic environment. Origin, distribution, assessment and toxicity effect for the aquatic biota, Ecohydrol. Hydrobiol. 21 (4) (2021) 655–668, https://doi.org/10.1016/j.ecohyd.2021.02.002.
[43] M. Matsuo, T. Tanaka, L. Ma, Gelation mechanism of agarose and κ-carrageenan solutions estimated in terms of concentration fluctuation, Polymer (Guildf). 43 (19) (2002) 5299–5309, https://doi.org/10.1016/S0032-3861(02)00290-2.
[44] P. Om, J. Nivedita, Immobilization of a thermostable MAmylase on agarose and agar matrices and its application in starch stain removal, World Appl. Sci. J. 13 (3) (2011) 572–577.
[45] W.-K. Lee, Y.-Y. Lim, A.-T.-C. Leow, P. Namasivayam, J. Ong Abdullah, C.-L. Ho, Biosynthesis of agar in red seaweeds: A review, Carbohydr. Polym. 164 (2017) 23–30, https://doi.org/10.1016/j.carbpol.2017.01.078.
[46] H. Sattar, A. Aman, S.A.U. Qader, Agar-agar immobilization: An alternative approach for the entrapment of protease to improve the catalytic efficiency, thermal stability and recycling efficiency, Int. J. Biol. Macromol. 111 (2018) 917–922, https://doi.org/10.1016/j.ijbiomac.2018.01.105.
[47] A.H. Clark, Structural and mechanical properties of biopolymer gels, Adv. Polym. Sci. 83 (1987) 57–192.
[48] J. Gille, R. Martin, J. Lubin, J.O. Larimer, Grayscale/Resolution Trade-Off for Text: Model Predictions and Psychophysical Results for Letter Confusion and Letter Discrimination, NASA. Published online, 1995.